

# Use of geoelectric and neutron methods to investigate water condition of the frozen ground, Mongolia

ISHIKAWA Mamoru<sup>1</sup>, SHARKHUU Natsagdorj<sup>2</sup>, DORJGOTOV Battogtokh<sup>2</sup>,  
BYAMBADEMBEREL D.<sup>2</sup>, KADOTA Tsutomu<sup>1</sup> and OHATA Tetsuo<sup>1</sup>

<sup>1</sup> Institute of Observational Research for Global Change, Yokohama, Japan

<sup>2</sup> Institute of Geography, MAS, Ulaanbaatar, Mongolia

*Key words: DC resistivity, frozen grounds, neutron probe, permafrost, unfrozen water*

## I Introduction

Soil water conditions are the crucial factor for characterizing frozen grounds. Most of the frozen ground contains both liquid and solid water. Ratio of unfrozen water controls the timing and magnitudes of geomorphic changes on permafrost-related landforms such as rock glacier and frost heaving, and land-surface hydrological components such as evapotranspiration, snow-melting infiltration and spring runoff. Estimating the contents of unfrozen water contents, therefore, has been the long lasting concerns by many hydro-geocryologists.

Although the great number of laboratory experiments has studied on this issue (*e.g.* Anderson *et al.*, 1973), there still remain lack of in-situ observations. Conventional time domain reflectometry (TDR) and sampling/drying methods are useful for estimating water contents at the shallower depths where the compositions of subsurface material are homogeneous. These methods are, however, not suitable for the deeper ground layers with large inhomogeneties. This is because that 1) sensor installation into deeper layers is significantly disturbs original soil textures, 2) periodic seasonal measurements by drying methods are also time-consuming and assume one-dimensionally bedded subsurface structures although this is not the case for the complex topography and subsurface conditions, and 3) TDR/drying methods measure water contents only neighboring sensors/sampling.

Instead, we attempted to apply direct current (DC) resistivity, neutron probing and their combination in the northeastern part of Mongolia. Time-lapse geophysical prospecting has recently known to be powerful tool for monitoring ground water condition at permafrost regions (*e.g.* Hauck *et al.*, 2002) and for agricultural purpose (*e.g.* Michot *et al.*, 2003). Three observational sites were selected as the representations, including flat pasture plain (FPP) at Nalaikh site, northern forested (NFS) and southern pasture slopes (SPS) near Terelj. Among these sites, permafrost were identified below the depth of 5.5 m at the Nalaikh site and 2.4 m at the northern slopes near Terelj settlement (Ishikawa *et al.*, 2003).

The current available data and analysis provided us some new aspects of hydro-thermal features of frozen ground in the southern boundaries of Eurasian discontinuous permafrost zone.

## II Data acquisitions

### 1. DC resistivity prospecting

The DC resistivity values of unconsolidated sediments are the function of the volumes of debris, pores, water and ice. The DC resistivity value of a frozen material is two or three orders of magnitude higher than that of an unfrozen material (*e.g.* Hoekstra and McNeill, 1973), because DC resistivity of ice are considerably higher than those of unfrozen water. Drying materials, containing high respective rate of air between soil particles, also show higher resistivity values, because air is nearly perfect electrical insulator.

The aims of DC resistivity methods are to investigate ground freezing and thawing condition. The electrode array (20 cm in unit electrode spacing) was inserted in the pre-drilled boreholes (89 mm in diameter). The depths of boreholes were determined to be 7 m at the FPP, 4 m at NFS and SPS sites, referring to active layer thicknesses (Ishikawa *et al.*, 2003). All boreholes were filled with fine sands in order to fix the electrode array and to insure good conductivities. The electrode layout is modified Pole-pole array. Subsurface electrode is for one set of current injection and voltage measurement. Another remote set was on the ground surface significantly far from the borehole.

The stacking type digital resistivity-meter, SYSCAL JUNIOR, was used for current injection and voltage measurements. This instrument is connected to remote control multiplexer, which determine four active electrodes and controls data sampling sequence through takeout-cables with number of relay circuits.

### 2. Neutron probe prospecting

Since the hydrogen molecular is in the form of water within the sediments, water contents can be estimated by counting the number of hydrogen molecules. Neutron probe method counts the number of hydrogen molecules and was used for estimating the volumetric water contents (VWC) in a sphere approximately 30 cm in diameter. The probe is composed of emitter and detector, and was inserted into access tube fixed in the pre-drilled borehole (89 mm in diameter). The borehole depths at each site were same as those for vertical resistivity measurements. Data readings were manually conducted at every 10 cm depth.

### III Theory for estimating unfrozen water contents of unsaturated soils

The neutron probe method determines the total contents of liquid and solid water. Accordingly, the combination with resistivity would enable us to estimate the volumetric rate of liquid and solid water. Relations between resistivity and water contents are formulated by Archie's empirical equation (Archie, 1942) for the unfrozen soils,

$$\rho_t = a\rho_{w,i}P^{-m}S_{w,t}^{-n} \quad (1)$$

and for the frozen soils,

$$\rho_f = a\rho_{w,f}P^{-m}\left(S_{w,f}\frac{\rho_{w,f}}{\rho_{w,i}}\right)^{-n} \quad (2)$$

where  $P$  is porosity,  $\rho_t$  and  $\rho_f$  are the resistivity of frozen, unfrozen soils,  $\rho_{w,i}$  and  $\rho_{w,f}$  are the resistivity of unfrozen water within frozen and unfrozen soils, respectively.  $S_{w,t}$  is and  $S_{w,f}$  are the fraction of the pore space occupied by liquid water, frozen and unfrozen soils.  $a$ ,  $n$  and  $m$  are empirically determined parameters. Rearranging eqs. (1) and (2), we obtain,

$$\frac{\rho_f}{\rho_t} = \left(\frac{S_{w,f}}{S_{w,t}}\right)^{-n} \left(\frac{\rho_{w,f}}{\rho_{w,i}}\right)^{1-n} \quad (3)$$

In partly frozen material, ionic transport still takes place in the liquid phase. Therefore resistivity depends strongly on the unfrozen water content  $S$  that is the fraction of water remaining unfrozen at subfreezing temperatures.  $S$  is given by (Daniel *et al.*, 1976),

$$S = \left(\frac{\rho_{w,f}}{\rho_{w,i}}\right) \quad (4)$$

For temperature below the freezing point resistivities increase exponentially until most of pore water is frozen, forming (McGinnis *et al.*, 1973)

$$\rho_f = \rho_i e^{b(T_f - T)} \quad (5)$$

where  $\rho_i$  is resistivity at the freezing point and  $b$  (in  $K^{-1}$ ) is constants. Substituting, eqs. (4) and (5) into (2), we obtain

$$S = \left(\frac{S_{w,f}}{S_{w,t}}\right)^{\frac{n}{1-n}} \exp\left\{\frac{b(T_f - T)}{1-n}\right\} \quad (6)$$

where  $T_f$  is the temperature at the freezing point.

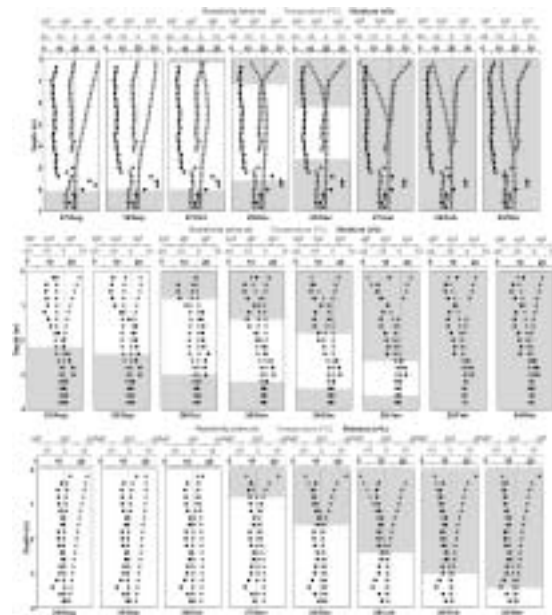
### IV Results and interpretations

Fig. 1 shows the once-per-month profile of DC resistivities and VWCs from August 2003 to March 2004, including ground temperature records at same date. Permafrost conditions were identified underneath FPP and NFS sites.

At the FPP site, neutron probing found extremely dry active layer with several v%. In spite of such less water contents, resistivities have significantly increased after temperature to be turned to negative, indicating phase change of soil water from liquid to solid. On the other hand, resistivities of permafrost layers almost remained to be less than those of active layer, even though soil water contents were high. This fact indicates that water of permafrost layer is unfrozen and that freezing/thawing phase change might not occur.

No permafrost was found at SPS site, where soil water contents were generally low with 10% for all depths. At this site, resistivity varied with temperatures and moistures. For the upper layers, resistivity increased with drying for unfrozen soils, and increased with further cooling of frozen soils. The latter is due to phase change of water as observed at FPP site.

The thawed layers of NFS site showed the most significant seasonal changes of moisture variations. For the summer period, the water between 2.2 and 2.6 m are probably liquid state, while those below 2.6 m are solid, as inspected by DC resistivity values. It was found that water contents significant increased were just above the thawing front. This indicates impermeabilities of frozen ground at this site. Beside, decreasing in DC resistivity values of frozen ground are probably due to increasing in



**Fig. 1 Resistivity, Temperature and Moisture at FPP (upper), NFS (middle) and SPS (lower) sites.**

unfrozen water. Such unfrozen water might be mobile and possibly migrated into overlying unfrozen layers. This consideration was from the fact that the VWCs below the depth 2.8 m slightly decreased especially from 19-Sep to 28-Oct when thawing front closed to permafrost table.

### V Determining soil-dependent parameters

Solution (6) requires the values of saturation component  $n$ , resistivity at freezing point  $\rho_i$  and  $b$ .  $n$  was estimated in order to fit measured and calculated resistivity for unfrozen soils ( $T > T_f$ ). Calculation uses following multiplicative equations of temperature- (*i.e.*  $f(T)$ ) and moisture-dependent (*i.e.*  $g(S_w)$ ) functions (Rein *et al.*, 2004),

$$\rho_t = \rho_i f(T) g(S_w) \quad (7)$$

where  $\rho_0$  is the resistivity measured at a reference temperature and moisture. A temperature-dependent function is given by;

$$f(T) = \frac{1}{1 + \alpha(T - T_0)} \quad (8)$$

where  $T_0$  is the reference temperature,  $\alpha$  is the temperature coefficient of resistivity ( $= 0.025 \text{ K}^{-1}$  for most electrolytes, Keller and Frischknecht, 1966).

The resistivities are also influenced by changing water content. Moisture-dependent function can be expressed by (Rein *et al.*, 2004);

$$g(S_w) = \left( \frac{S_w}{S_{w0}} \right)^{-n} \quad (9)$$

where  $S_{w0}$  is the reference degree of water saturation.

$\rho_i$  is simply determined by substituting parameter  $n$  into eq. (7). Finally  $b$  can be estimated by fitting eq. (5) to plots of resistivities versus subzero soil temperatures (Hauck, 2002).

Fig. 3 plots the parameters of  $n$ ,  $b$  and  $\rho_i$  with coefficients ( $a$ ) and their deviations ( $R^2$ ) for  $n$ . It was difficult to estimate these parameters for deeper layers at FPP site because of nearly no change in resistivities and temperatures. Among three sites SPS site showed the best correlations, in which  $a$  and  $R^2$  were nearly equal to 1. For the FPP site coefficients for the upper layers seem to be well, while those of lower were less than 0.5 in  $R^2$ , probably due to insignificant seasonal fluctuation both in resistivities and temperatures. Similarities occurred at NFS site, where coefficients ( $R^2$ ) at some depths were less than 0.5.

According to King *et al.* (1988),  $n$  mostly depend on grain sizes of soils, and tend to be larger for the finer soils. We found predominant  $n$  values were within 1 to 3,

which are in the coarse sand and silt categories. Considerably larger  $n$  values (more than 4) at FPP site probably indicate the presence of thin clay layers.

Exponential parameter  $b$  varied insignificantly with depths for NFS and SPS sites, ranging from 0.2 to 0.4  $\text{K}^{-1}$ . On the other hand,  $b$  at FPP sites increased from 0.2 to 3.5  $\text{K}^{-1}$  with depth, possibly due to the difference of initial water saturation (*e.g.* Hauck, 2002).

Resistivity at freezing point  $\rho_i$  can be simply determined by substituting above parameters into eq. (7). For this, it needs to input freezing points  $T_f$ , which may be estimated from plot of temperatures versus resistivities at each depth. They were ranged from -0.6 to -0.1  $^{\circ}\text{C}$ .

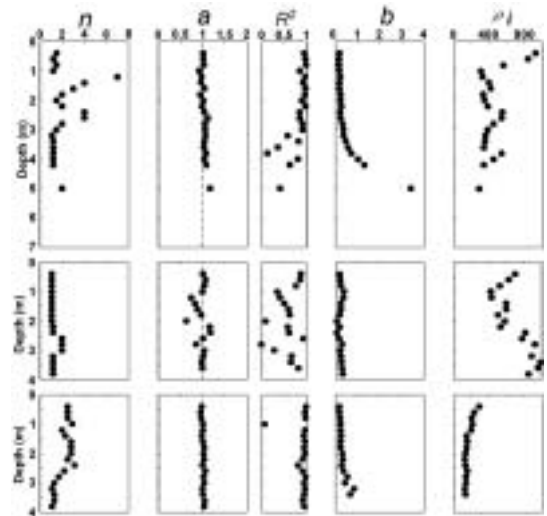


Fig. 2 Plots of soil-dependent parameters determined.

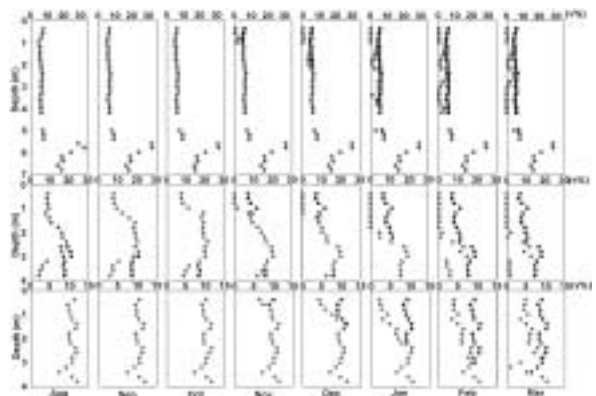


Fig. 3 Evolutions of unfrozen water contents at FPP (upper), NFS (middle) and SPS (lower) sites. Black dots shows the total water contents, the gray dots shows unfrozen water contents.

## VI Seasonal evolution of unfrozen water contents

Using eq. (6) and soil-dependent parameters determined, seasonal evolution of unfrozen water content were calculated at different depths for three sites (Fig. 3). Unfrozen water contents were dependent not only temperatures but also soil characteristics. The depths below 5.2 m at FPP site were assumed to be unfrozen throughout the period, since resistivities and temperatures did not vary seasonally. In spite of further cooling of soils at subzero temperatures, unfrozen water contents were nearly equal to total water contents at depths around 1.0 and 2.5 m, where finer grained soil layers might be presented.

Active layer at NFS site contains most water as ice especially mid- to late-winter. Greater contents of unfrozen water occurred at the uppermost layers of permafrost. On the contrary, 50 to 70% of total water was unfrozen at SPS site even in the mid-winter.

## VII Conclusions

The uses of DC resistivity and neutron probe methods, and their combination have large advantages for frozen ground investigation. They enable us to monitor in respective rates of liquid and solid water contents in the frozen grounds with high resolution and minimum artificial disturbance, covering deeper layers. Observations from summer to late-winter provided some new findings which include occurrences of unfrozen permafrost, impermeable role of frozen ground, water movements at the bottom of active layer and spatio-temporal variations of ground water conditions.

## References

Anderson, D. M., Tice, A. R., McKim, H. L. (1973): The unfrozen water and apparent specific heat capacity of frozen soils. in *North American Contribution, 2<sup>nd</sup> Int. Conf. on Permafrost*, Yakutsk, USSR., 289-295.

Archie, G. E. (1942): The electrical resistivity log as an aid in determining some reservoir characteristics. *Trans. Am. Inst. Min. Metall. Pet. Eng.*, **146**, 54-67.

Daniels, J. J, Keller, G. V, Jacobson, J. J. (1976): Computer-assisted interpretation of electromagnetic sounding over a permafrost section. *Geophysics.*, **41**, 752-765.

Hauck, C. (2002): Frozen ground monitoring using DC resistivity tomography. *Geophysical Research Letters*, **29** doi: 10.1029/2002GL014995.

Hoekstra, P., McNeill, D. (1973): Electromagnetic probing of permafrost. in: *North American contribution, Proc. 2<sup>nd</sup> Int. Conf. Permafrost*, 517-526.

Ishikawa, M., Sharkhuu, N., Zhang, Y., Kadota, T., Ohata, T. (2003): Spatial conditions of frozen ground and soil moisture at the southern boundary of discontinuous permafrost in Mongolia. in *8<sup>th</sup> ICOP Ext. Abst.*, Zurich, Switzerland., 67-68.

Keller, G. V., Frischknecht, F. C. (1966): *Electrical Methods in Geophysical Prospecting*. Pergamon Press Inc.

King, M. S., Zimmerman, W. and Corwin, R. F. (1988): Seismic and electrical profiles of unconsolidated permafrost. *Geophysical Prospecting*, **36**, 349-364.

McGinnis, L. D., Nakano, K., Clark, C. C. (1973): Geophysical identification of frozen and unfrozen ground, Antarctica. in *Proc. 2<sup>nd</sup> Int. Conf. Permafrost*, Yakutsk, USSR, 136-146.

Michot, D., Benderitter, Y., Nicoullaud, B., King, D., Tabbagh, A. (2003): Spatial and temporal monitoring of soil water content with an irrigated corn crop cover using surface electrical resistivity tomography. *Water Resources Research*, **39**, doi:10.1029/2002WR001581.

Rein, A., Hoffmann, R., Dietrich, P. (2004): Influence of natural time-dependent variation of electrical conductivity on DC resistivity measurements. *Journal of Hydrology*, **285**, 215-232.